

Impact of Environmental Instability on Convective Precipitation Uncertainty Associated with the Nature of the Rimed Ice Species in a Bulk Microphysics Scheme

KWINTEN VAN WEVERBERG

Brookhaven National Laboratory, Upton, New York, and Université Catholique de Louvain, Louvain-la-neuve, Belgium

(Manuscript received 25 January 2013, in final form 16 April 2013)

ABSTRACT

Despite a number of studies dedicated to the sensitivity of deep convection simulations to the properties of the rimed ice species in microphysics schemes, no consensus has been achieved on the nature of the impact. Considering the need for improved quantitative precipitation forecasts, it is crucial that the cloud modeling community better understands the reasons for these differing conclusions and knows the relevance of these sensitivities for the numerical weather prediction. This study examines the role of environmental conditions and storm type on the sensitivity of precipitation simulations to the nature of the rimed ice species (graupel or hail). Idealized 3D simulations of supercells/multicells and squall lines have been performed in varying thermodynamic environments. It has been shown that for simulation periods of sufficient length (>2 h), graupel-containing and hail-containing storms produce domain-averaged surface precipitation that is more similar than many earlier studies suggest. While graupel is lofted to higher altitudes and has a longer residence time aloft than hail, these simulations suggest that most of this graupel eventually reaches the surface and the surface precipitation rates of hail- and graupel-containing storms converge. However, environmental conditions play an important role in the magnitude of this sensitivity. Storms in large-CAPE environments (typical of storms in the U.S. Midwest) are more sensitive than their low-CAPE counterparts (typical of storms in Europe) to the nature of the rimed ice species in terms of domain-average surface precipitation. Supercells/multicells are more sensitive than squall lines to the nature of the rimed ice species in terms of spatial precipitation distribution and peak precipitation, disregarding of the amount of CAPE.

1. Introduction

The advent of high-resolution cloud-resolving models over the past decades has allowed model developers to remove the deep convective parameterization in numerical weather prediction (NWP). However, in so doing, it also further exposed uncertainties within the remaining parameterizations. Surface precipitation from idealized supercell simulations, for instance, has been shown to be larger by a factor of 2–4 in simulations when the rimed ice species (RIS) in the microphysics parameterization is fast falling (i.e., hail) as opposed to slowly falling (i.e., graupel) [Gilmore et al. (2004, hereafter GSR04); van den Heever and Cotton (2004); Morrison and Milbrandt (2011, hereafter MM11)]. However, such

sensitivity was found to be much less pronounced in studies on idealized squall-line simulations (Van Weverberg et al. 2012a; Bryan and Morrison 2012), and in real-case simulations (Reinhardt and Seifert 2006; Van Weverberg et al. 2011, 2012b).

Given the need for more accurate precipitation simulations, it is crucial to understand the reasons for the considerable variability in sensitivities found among previous studies, and to better understand their relevance to the operational weather forecasts. The question arises whether supercells seem to be more responsive to changes in RIS than squall lines because of the specific environmental conditions, the different dynamics of supercells versus squall lines, or because of differences in the numerical aspects of the respective studies, such as domain setup or length of the simulation. Van Weverberg et al. (2012b) found this sensitivity to correlate with the environmental instability in real-case simulations of deep convection. To further explore this hypothesis, this paper examines the role of environmental conditions and storm type on the sensitivity of surface precipitation to the

Corresponding author address: Kwinten Van Weverberg, Université catholique de Louvain, Georges Lemaître Centre for Earth and Climate Research, SC10-L4.03.08 Mercator, Place Louis Pasteur 3, Louvain-la-Neuve, 1348, Belgium.
E-mail: kwinten.vanweverberg@uclouvain.be

nature of the rimed ice. To do so, idealized 3D sensitivity simulations of squall lines and supercells have been performed using two different thermodynamic environments. The next section describes the model setup and the experimental design. Results are documented in section 3 and summarized in section 4.

2. Model description and experiment design

a. Model description

The Advanced Research Weather Research and Forecasting Model (ARW-WRF) version 3.2 (Skamarock et al. 2007) was used for all experiments in this study, which is a fully compressible, nonhydrostatic three-dimensional cloud model. Idealized simulations of squall lines and supercells were performed. The squall-line simulations had open boundary conditions in the across-line direction, and periodic boundary conditions in the along-line direction. The supercell simulations had open boundaries in all directions. All simulations had a 1-km horizontal grid spacing, and 40 vertical levels with 500-m spacing. The horizontal domain was 350 km \times 350 km for the supercell simulations, and 400 km \times 100 km for the squall-line simulations. Turbulence was represented by a 1.5-order turbulent kinetic energy scheme and radiation, boundary layer, and surface processes were turned off. The model was integrated for 5 h in all simulations. The supercell was initialized using the analytic sounding of Weisman and Klemp (1982) and the quarter-circle hodograph of Weisman and Rotunno (2000). Convection was triggered using a thermal perturbation of maximum 3 K centered at a height of 1.5 km. The squall line was integrated using the same temperature and moisture sounding, but with a vertical wind shear of 0.0048 s⁻¹ in the lowest 2.5 km and no shear above. Convection was initiated using a linear cold pool, as in Bryan and Morrison (2012). While the supercell environment typically does not only produce supercells, but rather a mixture of supercells, multicells, and bow echoes, these simulations will be referred to as “supercells” in the remainder of this paper for brevity. Hence, the supercells in all further analysis include the totality of this mixture of storm types (consistent with earlier studies, e.g., GSR04; MM11).

b. Experiment design

All simulations were performed using the Morrison et al. (2009) bulk two-moment microphysics scheme, which predicts the number concentration and mixing ratio of cloud water, ice, rain, snow, and graupel. The aerosol distribution and cloud droplet activation was treated as in Solomon et al. (2011). Inverse exponential functions were assumed for all precipitation size distributions. Mass and number-concentration-weighted

TABLE 1. Experiment overview. Provided for each experiment are the rimed ice density (ρ_H), the coefficient (a_{vx}), and exponent (b_{vx}) in Eq. (1) for the rimed ice species, the CAPE, and the storm type.

Expt	ρ_H (kg m ⁻³)	a_{vx}	b_{vx}	CAPE (J kg ⁻¹)	Storm type
SQ-G-1000	400	19.3	0.37	1000	Squall line
SQ-H-1000	900	114.5	0.50	1000	Squall line
SQ-G-3000	400	19.3	0.37	3000	Squall line
SQ-H-3000	900	114.5	0.50	3000	Squall line
SU-G-1000	400	19.3	0.37	1000	Supercell
SU-H-1000	900	114.5	0.50	1000	Supercell
SU-G-3000	400	19.3	0.37	3000	Supercell
SU-H-3000	900	114.5	0.50	3000	Supercell

bulk fall velocities for all hydrometeors are calculated using power-law velocity–diameter relationships:

$$V_x(D) = a_{vx} D^{b_{vx}}, \quad (1)$$

where a_{vx} and b_{vx} are empirically derived constants. Two sets of microphysics experiments were performed; one assuming graupel (G) as the RIS and the other assuming hail (H). Characteristics of the RIS were modified to represent either graupel or hail by adjusting the bulk particle density and the a_{vx} and b_{vx} fall speed parameters, as outlined in Table 1.

To understand how thermodynamic instability affects the difference between the simulations that contain graupel or hail, modifications were applied to the Weisman and Klemp (1982) sounding to obtain environments with two different amounts of convective available potential energy (CAPE), being 1000 and 3000 J kg⁻¹. To do so, the temperature profile was modified using a sinusoidal perturbation to the temperature of the original sounding above the freezing level (4000 m) with a maximum temperature adjustment at the 8000-m level. The water vapor profile was modified accordingly to keep the relative humidity identical to the initial sounding. This approach produced profiles with different amounts of CAPE, while the freezing level and the lifted condensation level were identical for the different soundings. The soundings used in all experiments, as well as the amount of CAPE, are depicted in Fig. 1. A total of eight experiments (listed in Table 1) result from the combination of two different environmental instability conditions with two different settings for the RIS for the squall-line and supercell/multicell simulations.

3. Results

a. Surface precipitation accumulations

In contrast to many previous idealized studies, our simulations show a smaller difference of precipitation

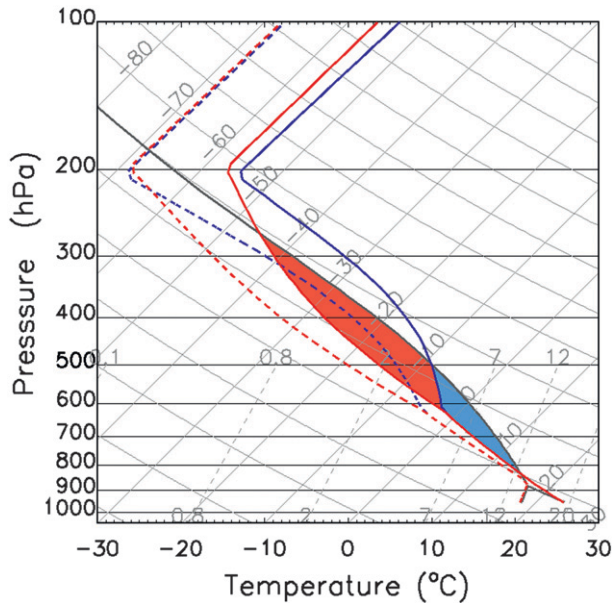


FIG. 1. Initial vertical profiles of temperature (solid colored lines) and dewpoint temperature (dashed colored lines) for all simulations. Blue (red) lines are for the low-CAPE (high CAPE) soundings. The blue (red + blue) area indicates the amount of CAPE in the low-CAPE (high CAPE) sounding.

fallout between the G and H simulations (Table 2). (Differences between the G and H simulations are hereafter referred to as ΔGH .) Fairly small ΔGH s are found between the simulations with limited CAPE (SQ-1000, SU-1000) over the 5-h accumulation time. For the large CAPE simulations, the domain-averaged precipitation ΔGH is more pronounced. A squall line that contains hail (SQ-H-3000) rather than graupel (SQ-G-3000) produces about 20% more surface precipitation. The squall line simulated by Bryan and Morrison (2012) showed a similar

domain-averaged precipitation ΔGH . Our high-CAPE supercell simulation with hail (SU-H-3000) has about 45% more surface precipitation compared to the simulation with graupel (SU-G-3000), which is a much smaller response than in the supercells simulated by GSR04 and MM11, despite similar atmospheric environments.

In the squall lines, the nature of the RIS does not seem to matter much for the spatial distribution of the surface precipitation for both low- and high-CAPE environments, although higher precipitation values occur near the leading edge of the squall in SQ-H-3000 than in SQ-H-3000 (Figs. 2a–d). Conversely, for supercells the structure of the precipitation field is largely affected by the choice between graupel and hail (Figs. 2e–h). Supercells that contain graupel produce a much broader precipitation area and much smaller peak rain rates, as can also be derived from the 95th percentiles of the accumulated precipitation in Table 2. This is even true for the low-CAPE supercells and is consistent with GSR04 and van den Heever and Cotton (2004).

b. Temporal storm evolution

Figure 3 shows the temporal evolution of the key components of the water balance in the experiments. The ΔGH for precipitation rates in SQ-1000 is very small throughout the simulations (black dashed lines). The SQ-G-3000, however, exhibits a delay in precipitation onset of about half an hour compared to SQ-H-3000. In the supercells, the slower onset of precipitation fallout becomes more important and the G and H precipitation rates do not converge until after 3 h of simulation time in SU-1000 and after 5 h in SU-3000.

Since all previous studies that report a large ΔGH sensitivity of the domain-averaged precipitation accumulations in supercell environments were integrated for only

TABLE 2. Statistics for all eight experiments after 5 h of simulation. (from left to right) Domain-averaged 5-h accumulated surface precipitation (mean), the 95th percentile of the domain-average 5-h accumulated precipitation (95%), the precipitation efficiency (PE; percentage of consumed vapor that ends up as surface precipitation after 5 h), the vapor gain (percentage of consumed vapor that is returned by evaporation or sublimation after 5 h), storage (percentage of consumed vapor that ends up as clouds and precipitation aloft after 5 h), domain-maximum vertical velocity, averaged over all available output times (W), the time- and domain-averaged updraft mass flux (UMF; for vertical velocity $>1 \text{ m s}^{-1}$), the time-averaged total cold pool area (CPA; cold pools are defined as regions with perturbation temperature $<-2 \text{ K}$), and the time- and cold pool-averaged cold pool intensity (CPI, defined as in Weisman and Rotunno 2004).

Expt	Mean (mm)	95% (mm)	PE (%)	Vapor gain (%)	Storage (%)	W (m s^{-1})	UMF ($10^{10} \text{ kg s}^{-1}$)	CPA (10^3 km^2)	CPI (m s^{-1})
SQ-G-1000	6.5	32.2	40	53	7	11.6	7.9	18.4	24.0
SQ-H-1000	6.7	36.2	41	53	6	11.6	7.9	18.6	23.7
SQ-G-3000	12.2	47.2	32	55	13	28.1	18.3	19.7	30.3
SQ-H-3000	14.8	49.9	38	51	11	27.5	17.9	20.7	27.1
SU-G-1000	2.2	38.7	37	45	18	32.6	12.3	6.1	12.9
SU-H-1000	2.4	62.3	46	39	15	31.5	12.0	8.9	12.2
SU-G-3000	4.9	19.5	18	54	28	55.5	52.0	10.5	14.2
SU-H-3000	7.1	27.4	34	45	21	56.4	42.8	14.6	15.7

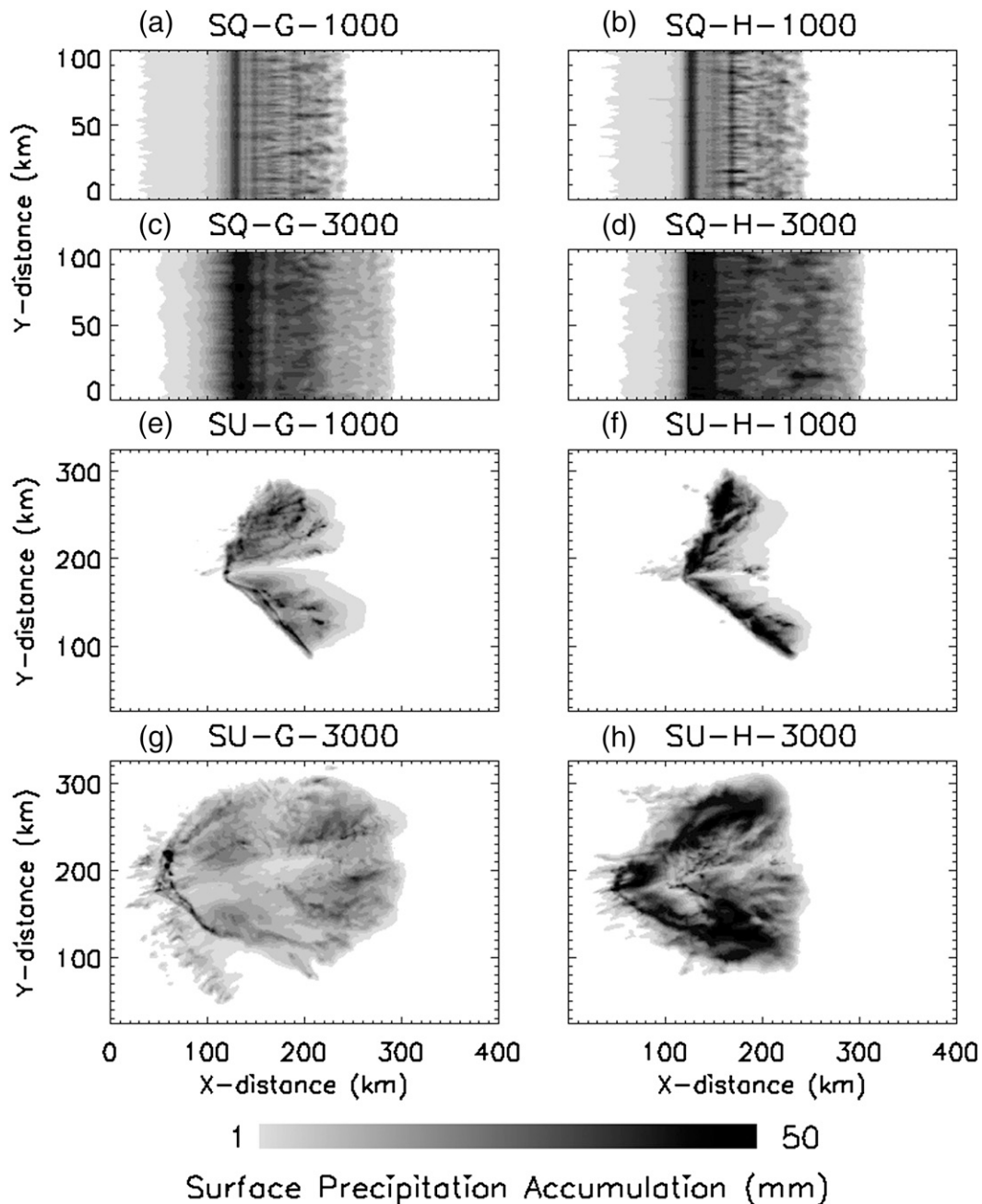


FIG. 2. Spatial distribution of the 5h accumulated surface precipitation in all experiments. Colorbar is a linear scale.

2 h (GSR04; MM11), they only picked up on the early delayed precipitation onset, but largely missed the gradual convergence in precipitation rates after this time (Figs. 3c,d). After only 2 h in our simulations, the H supercells also produce up to 3 times the surface precipitation than G supercells (see insets).

The other components depicted in Fig. 3 provide insight into the entire water vapor balance of the simulations. Water vapor can be lost to (i.e., consumed by) clouds by

condensation and deposition (red solid lines). Once consumed by the microphysics scheme, water vapor can eventually end up as surface precipitation (black dashed lines), stored aloft as clouds (black asterisks), or be returned to vapor by evaporation or sublimation (blue lines).

The delayed onset of precipitation in SQ-G-3000 compared to SQ-H-3000 (Fig. 3b) is related to there being more water stored in clouds in SQ-G-3000 (black

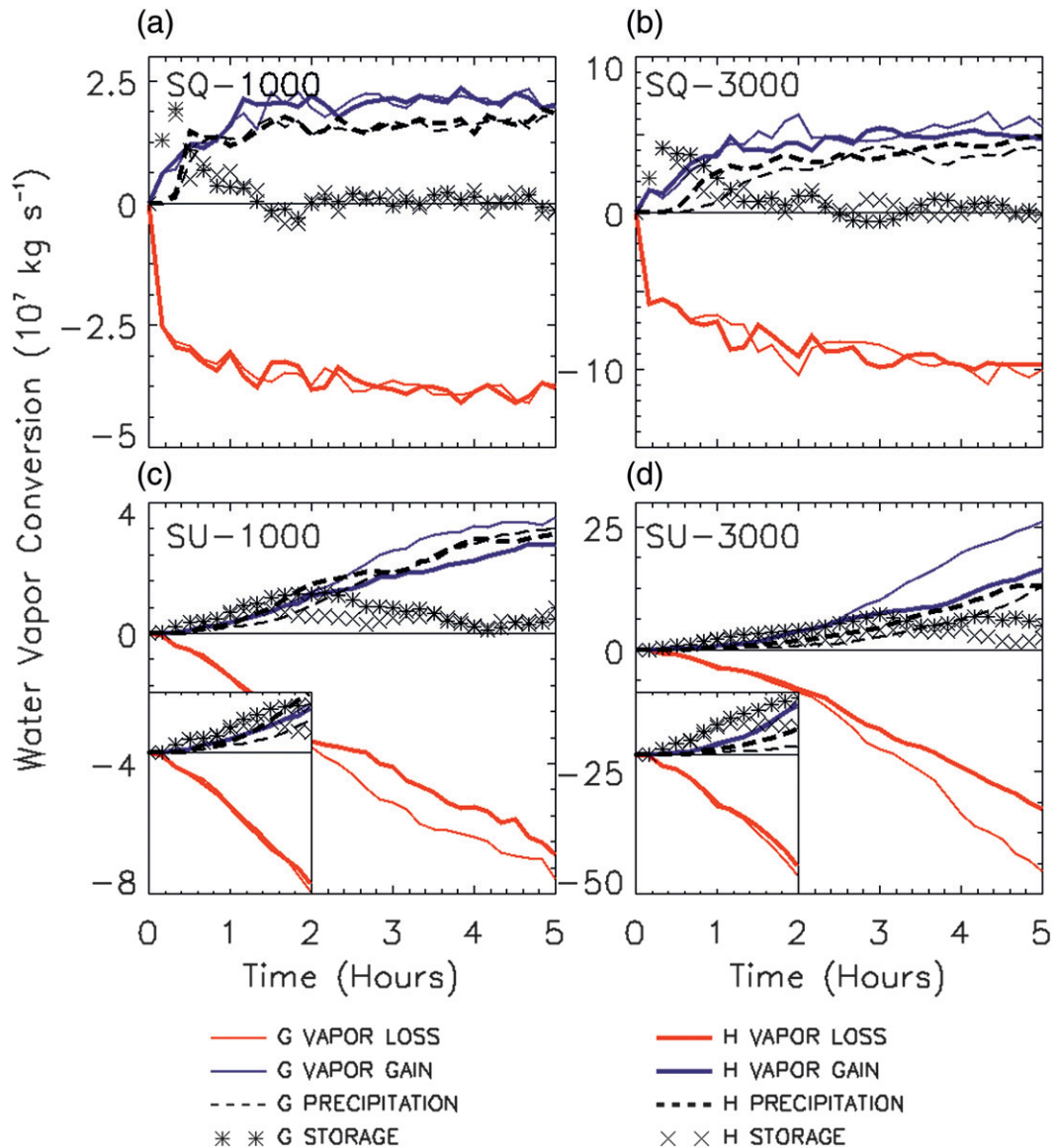


FIG. 3. Time series for the entire simulations of the (a) SQ-1000, (b) SQ-3000, (c) SU-1000, and (d) SU-3000 experiments. Shown are the domain-total surface precipitation rate (precipitation), domain-total change in cloud and precipitation mass aloft (storage), domain-total vapor loss (condensation and deposition), and domain-total vapor gain (evaporation and sublimation). The graupel experiments are denoted by thin lines and the hail experiments by thick lines. The insets in the SU-experiments provide an enlarged view of the first two simulation hours for clarity.

asterisks). All squall-line simulations reach equilibrium rather soon after initiation, reflected in a zero change in storage of water in clouds and almost constant vapor consumption after 1.5 h (Figs. 3a,b). In contrast, supercells do not reach equilibrium. The cold pools continue to spread throughout the simulation and triggering more multicells and supercells (not shown). Even after 5 h, the supercells continue to store more water into clouds (i.e., the total cloud mass increases) and consume more vapor (Figs. 3c,d). The difference in precipitation rates between the SU-G and SU-H experiments, mainly early in the

simulation, are related again to a change in the amount of water that is stored in clouds. Because of its slower fall velocity, graupel is retained aloft longer (not shown), leading to a larger cloud buildup and less surface precipitation. Later into the simulation, graupel eventually reaches the surface and the G and H precipitation rates converge.

c. Water vapor budget analysis

Another feature that emerges from Fig. 3 is the larger vapor consumption in SU-G compared to SU-H. Despite

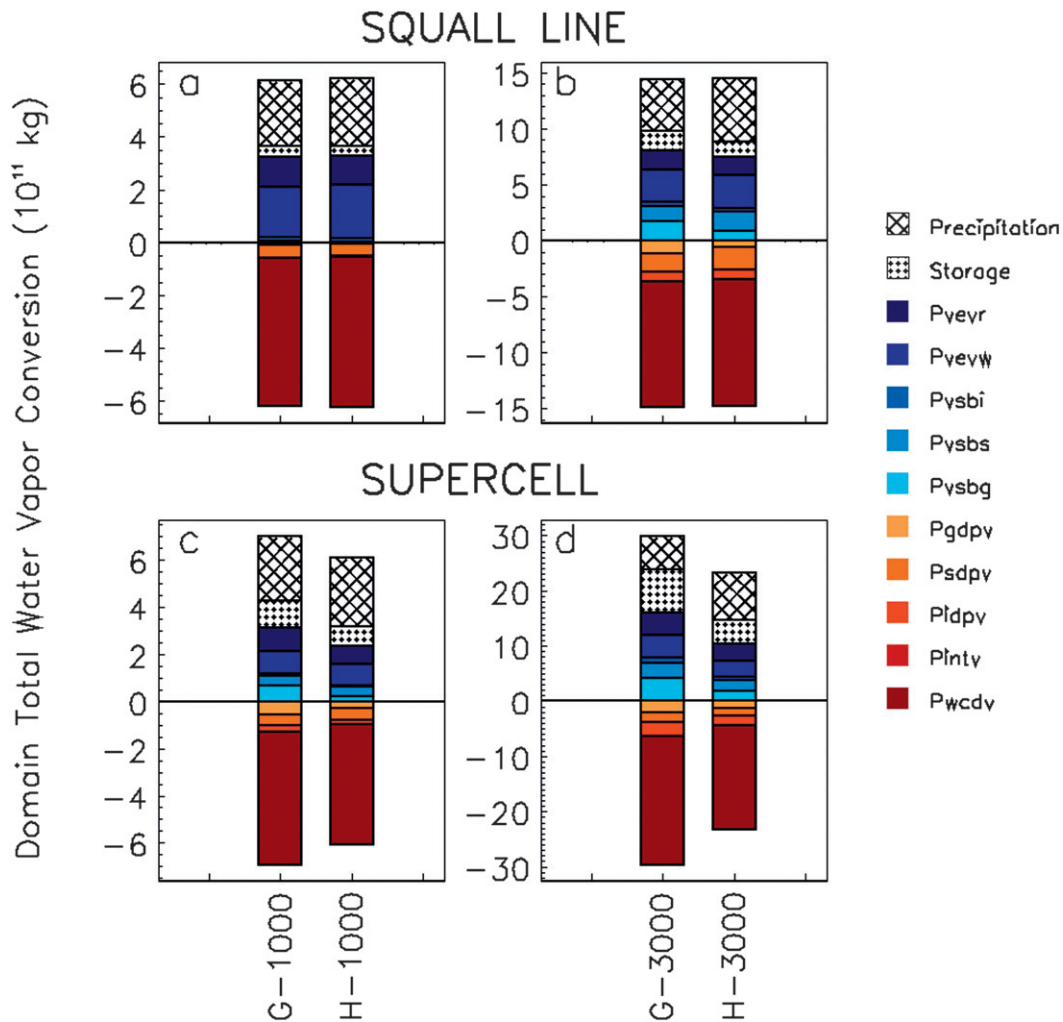


FIG. 4. (a)–(d) Domain- and time-integrated water vapor budgets for all experiments. Negative values (red colors) are the vapor loss and positive values (blue colors) are the vapor gain. The specific processes are denoted with the acronyms in the legend and are further explained in the appendix. The hatched bars denote the total amount of vapor that becomes surface precipitation at the end of the simulation time, and the dotted bars denotes the total amount of vapor that remains stored in clouds and precipitation aloft. The proportion of the precipitation (hatched bars) to the vapor loss (red bars) gives the precipitation efficiency.

the smaller/delayed precipitation fallout in the SU-G experiments, they consume considerably more water vapor. Figure 4 provides an overview of the specific source and loss terms of water vapor accumulated for the entire simulation periods. To provide a complete water vapor budget, the total surface precipitation and total water mass that is stored in the clouds are added. In the squall-line simulations, the nature of the RIS (G or H) has no impact on the amount of vapor consumed (red bars in Fig. 4). In SQ-1000, equal amounts of the total condensed water mass in the G and H experiments end up in clouds (storage), surface precipitation, and vapor gain (blue bars in Fig. 4). In SQ-3000, more graupel sublimation (Pvsbg) takes place in the G than in the H experiment, and a larger amount of condensed water remains stored aloft.

This leaves less water for surface precipitation and explains the slightly lower accumulations in SQ-G-3000 than in SQ-H-3000.

The supercells exhibit a different picture. As outlined above and consistent with GSR04 and Van Weverberg et al. (2011), the G experiments consume more vapor than the H experiments, mainly by cloud condensation and graupel deposition (red bars in Figs. 4c,d). The vapor consumption in the G and H supercell experiments mainly start to diverge after 2 h (Figs. 3c,d). Since graupel is lofted to higher altitudes than hail, it is picked up by the upper-level outflow and dragged into the anvil region ahead of the main storm system. After about 2 h, graupel reaches the surface ahead of the main updrafts in the G experiments and starts to inhibit rapid cold

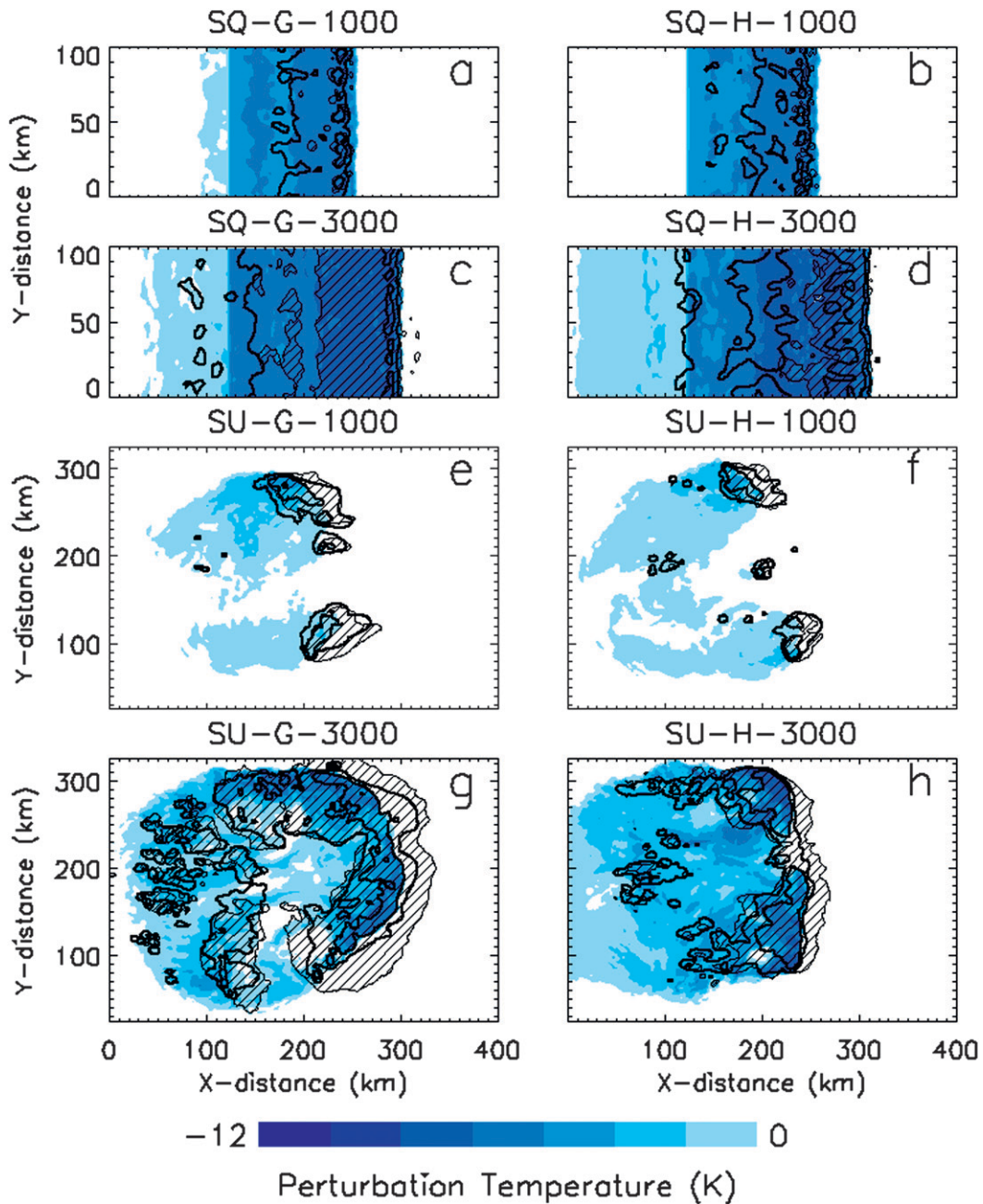


FIG. 5. (a)–(h) Horizontal cross sections for all the experiments 5 h into the simulation. The color shading indicates the cold pool intensity, clouds are indicated with the hatched area (vertically integrated condensed water path $>5 \text{ g m}^{-2}$), and the black contours denote surface precipitation (contours at 10^{-4} , 10^{-3} , and $10^{-2} \text{ kg m}^{-3}$).

pool growth at the leading edge of the storm system (not shown). Figure 5 denotes horizontal cross sections through the storm systems and their associated cold pools, 5 h into the simulation. By that time, the G supercells have propagated farther eastward than the H supercells (Figs. 5e–h), despite their weaker cold pools and smaller total cold pool area (Table 2). It is likely that the faster (but less intense) cold pools force more air into saturation

in the G supercells compared to the H supercells. Note that this mechanism cannot be reproduced in the squall-line simulations because of the deep cold pool that was imposed to initiate the convection (Figs. 5a–d).

Since more condensate resides aloft a longer time in the SU-G experiments, more condensate is also depleted by sublimation and evaporation, instead of raining out to the surface (Figs. 3 and 4). Hence, precipitation

efficiencies (PE) in SU-G are significantly lower than in SU-H (Table 2). In SU-G-1000 the decrease in PE compensates for the additional vapor consumption resulting in equal amounts of surface precipitation as in SU-H-1000. In SU-3000, the reduction in PE in the G as opposed to the H experiment is so large that it overcompensates for the excess vapor consumption in the G experiment (Fig. 4 and Table 2) and, hence, results in the smaller surface precipitation accumulation in G.

4. Conclusions

Considering the need for more accurate quantitative precipitation forecasts, it is crucial that the sensitivities of deep convective simulations to assumptions in the microphysics parameterization are better understood. Despite a number of studies dedicated to understand the role of the rimed ice species (RIS) in the precipitation forecast, no consensus has been achieved on the nature of the impact. Studies on idealized supercell/multicell simulations typically report that storms simulated with the RIS typical of hail have precipitation fallout that is 2–4 times larger than when graupel is treated (GSR04; MM11). Conversely, studies on squall-line simulations often report limited sensitivity (Bryan and Morrison 2012) or no sensitivity at all (Van Weverberg et al. 2011).

We have shown that the very large sensitivity of domain-averaged precipitation in studies on intense supercell/multicell storms is largely due to delayed precipitation onset when the RIS is typical of graupel rather than hail. These studies typically performed short simulations and, hence, are mainly relevant for very short-range NWP (in the order of a few hours), since the impact of the choice of graupel or hail fades when the entire convective cycle is considered. However, the choice of graupel versus hail affects the spatial distribution of precipitation fallout and the peak precipitation rates in supercells/multicells, even after longer integration times and for low-CAPE environments.

We further demonstrated that the role of the RIS on surface precipitation varies significantly with the environmental conditions. The larger the CAPE, the more significant the Δ GH sensitivity of the domain-averaged surface precipitation becomes. Also, the supercell environment seemed more sensitive to the RIS than the squall-line environment. High-CAPE supercells/multicells produced about 45% more surface rainfall when they contained hail rather than graupel. Conversely, low-CAPE squall lines were insensitive to the nature of the RIS. In the more energetic storm systems, graupel was lofted to higher altitudes than hail and a larger fraction of the condensate was sublimated, evaporated, or remained stored aloft at the end of the simulation time.

We further noted a significant difference between the squall-line and the supercell/multicell behaviors. Squall lines quickly reach equilibrium and there is little difference between the graupel-containing and hail-containing squall lines in terms of vertical structure or total vapor consumption. Supercells, however, do not reach equilibrium during the 5-h simulation and continue to grow larger. Graupel-containing supercells/multicells also consume much more water vapor than hail-containing supercells/multicells. This is likely related to faster cold pool propagation (despite weaker cold pools) in the graupel-containing supercells, forcing more air into saturation than the hail-containing supercells. Since our squall lines were initiated with a strong cold pool, storm propagation was determined more by the imposed cold pool than by additional cooling due to graupel/hail melting and the above mechanism could not be reproduced for the squall-line simulations.

Although our simulations of the supercell/multicell storms were longer than those by previous studies that reported a stronger sensitivity of surface precipitation, they still did not cover the full convective cycle of the storms. Limitations in computation time still constrain the simulations of supercells to limited domains and integration times, but it should be investigated how responsive storms are when their entire lifetime is concerned. It is likely that the significance of the choice of graupel or hail further decreases at later stages of the convective cycle.

Furthermore, since sublimation of graupel seems to determine the differences in precipitation efficiencies between the graupel- and hail-containing storms, an important factor might also be the relative humidity within the storm environment. Drier environmental conditions should lead to more sublimation of graupel and, hence, a larger sensitivity to the choice of the RIS. Future studies should take this into account. Also, recently, schemes have been developed that include both hail and graupel and hence do not require modelers to choose between either graupel or hail (Milbrandt and Yau 2005; Mansell et al. 2010). However, Van Weverberg et al. (2012a) suggested that large uncertainties still exist within such schemes related to the graupel-to-hail conversion. It should be investigated how the uncertainties related to the graupel-to-hail conversion in schemes with two RIS compare with uncertainties associated with the choice of either graupel or hail in schemes that contain a single RIS.

Acknowledgments. This research was supported by the U.S. Department of Energy's Atmospheric System Research (ASR), an Office of Science Program, and by the Earth System Modeling Program via the Fast-Physics System Testbed and Research (FASTER) project

(www.bnl.gov/esm). The author is grateful to Andy M. Vogelmann for stimulating discussions and to H. Morrison for assistance with the cold pool initiation of the squall-line simulations.

APPENDIX

Conversion Term Abbreviations

The abbreviations used in Fig. 4 are constructed so that the second letter is the category experiencing the gain, and the last letter is the category experiencing the loss. The third and fourth letters indicate the process associated with the conversion: ev (evaporation), cd (condensation), sb (sublimation), dp (deposition), and nt (initiation).

Pvevr	Rain evaporation
Pvevw	Cloud water evaporation
Pvsbi	Cloud ice sublimation
Pvsbs	Snow sublimation
Pvsbg	Hail/graupel sublimation
Pgdvp	Hail/graupel depositional growth
Psdpv	Snow depositional growth
Pidpv	Cloud ice depositional growth at the expense of water vapor
Pintv	Initiation of cloud ice at the expense of water vapor
Pwcdv	Cloud water condensation

REFERENCES

- Bryan, G. H., and H. Morrison, 2012: Sensitivity of a simulated squall line to horizontal resolution and parameterization of microphysics. *Mon. Wea. Rev.*, **140**, 202–225.
- Gilmore, M. S., J. M. Straka, and E. N. Rasmussen, 2004: Precipitation uncertainty due to variations in precipitation particle parameters within a simple microphysics scheme. *Mon. Wea. Rev.*, **132**, 2610–2627.
- Mansell, E. R., C. L. Ziegler, and E. C. Brunning, 2010: Simulated electrification of small thunderstorm with two-moment bulk microphysics. *J. Atmos. Sci.*, **67**, 171–194.
- Milbrandt, J. A., and M. K. Yau, 2005: A multimoment bulk microphysics parameterization. Part II: A proposed three-moment closure and scheme description. *J. Atmos. Sci.*, **62**, 3065–3081.
- Morrison, H., and J. A. Milbrandt, 2011: Comparison of two-moment bulk microphysics schemes in idealized supercell thunderstorm simulations. *Mon. Wea. Rev.*, **139**, 1103–1130.
- , G. Thompson, and V. Tatarskii, 2009: Impact of cloud microphysics on the development of trailing stratiform precipitation in a simulated squall line: Comparison of one- and two-moment schemes. *Mon. Wea. Rev.*, **137**, 991–1007.
- Reinhardt, T., and A. Seifert, 2006: A three-category ice scheme for LMK. *COSMO Newsl.*, **6**, 115–120.
- Skamarock, W. C., J. B. Klemp, J. Dudhia, D. O. Gill, D. M. Barker, W. Wang, and J. G. Powers, 2007: A description of the Advanced Research WRF version 2. NCAR Tech. Note NCAR/TN-468+STR, 88 pp.
- Solomon, A., M. D. Shupe, P. O. G. Persson, and H. Morrison, 2011: Moisture and dynamical interactions maintaining decoupled Arctic mixed-phase stratocumulus in the presence of a humidity inversion. *Atmos. Chem. Phys.*, **11**, 10 127–10 148.
- van den Heever, S. C., and W. R. Cotton, 2004: The impact of hail size on simulated supercell storms. *J. Atmos. Sci.*, **61**, 1596–1609.
- Van Weverberg, K., N. P. M. van Lipzig, and L. Delobbe, 2011: The impact of size distribution assumptions in a simple microphysics scheme on surface precipitation and storm dynamics during a low-topped supercell case. *Mon. Wea. Rev.*, **139**, 1131–1147.
- , A. M. Vogelmann, H. Morrison, and J. A. Milbrandt, 2012a: Sensitivity of idealized squall line simulations to the level of complexity used in two-moment bulk microphysics schemes. *Mon. Wea. Rev.*, **140**, 1883–1907.
- , N. P. M. van Lipzig, L. Delobbe, and A. M. Vogelmann, 2012b: The role of precipitation size distributions in km-scale NWP simulations of intense precipitation: Evaluation of cloud properties and surface precipitation. *Quart. J. Roy. Meteor. Soc.*, **138**, 2163–2181.
- Weisman, M. L., and J. B. Klemp, 1982: The dependence of numerically simulated convective storms on vertical wind shear and buoyancy. *Mon. Wea. Rev.*, **110**, 504–520.
- , and R. Rotunno, 2000: The use of vertical wind shear versus helicity in interpreting supercell dynamics. *J. Atmos. Sci.*, **57**, 1452–1472.
- , and —, 2004: “A theory for long-lived squall lines” revisited. *J. Atmos. Sci.*, **61**, 361–382.